

1 **Multiscale regression model to infer historical**  
2 **temperatures in a central Mediterranean Sub-regional**  
3 **Area**

4

5 **N. Diodato<sup>1</sup>, G. Bellocchi<sup>1,2</sup>, C. Bertolin<sup>3</sup>, and D. Camuffo<sup>3</sup>**

6

7 <sup>1</sup>MetEROBS – Met European Research Observatory, GEWEX-CEOP Network, World Climate Research  
8 Programme, via Monte Pino snc, 82100 Benevento, Italy

9 <sup>2</sup>Grassland Ecosystem Research Unit, French National Institute of Agricultural Research, avenue du Brézet  
10 234, 63000 Clermont-Ferrand, France

11 <sup>3</sup>Atmosphere and Ocean Science Institute, National Research Council of Italy, corso Stati Uniti 4, 35127  
12 Padua, Italy

13 **Abstract**

14

15 This paper has exploited, for Southern and Central Italy (Mediterranean Sub-Regional  
16 Area), an unprecedented historical dataset as an attempt to model seasonal (winter and  
17 summer) air temperatures in pre-instrumental time (back to 1500). Combining information  
18 derived from proxy documentary data and large-scale simulation, a statistical downscaling  
19 approach in the form of multiscale–temperature regression (MTR)–model was developed to  
20 adapt larger-scale estimations (regional component) to the sub-regional temperature pattern  
21 (local component). It interprets local temperature anomalies by means of monthly-based  
22 Temperature Anomaly Scaled Index in the range -5 (very cold conditions in June) to 2  
23 (very warm conditions). The modelled response agrees well with the independent data  
24 from the validation sample (Nash-Sutcliffe efficiency coefficient >0.60). The advantage  
25 of the approach is not merely increased accuracy in estimation. Rather, it relies on the  
26 ability to extract (and exploit) the right information to replicate coherent temperature  
27 series in historical times.

28

## 29 1 Introduction

30  
31 Modelling can be described as an art because it involves experience and intuition as well as  
32 the development of a set of – mathematical - skills.

33  
34 Mark Mulligan and John Wainwright (eds.), 2004. *Environmental Modelling*, Wiley, Chichester, p. 8.

35  
36 The Mediterranean is one of the few regions in the world holding a large volume of  
37 weather documentary proxies for the past 500-1000 years (Camuffo and Enzi, 1992;  
38 Jones et al., 2009). However, such large amounts of documents and archives have not yet  
39 been fully explored to reproduce with high spatio-temporal resolution the different  
40 climates of Mediterranean (García-Herrera et al., 2007). Determining the climatic history  
41 in these unrepresented places of the world is a challenging and complex issue at both  
42 theoretical and applicative levels.

43 Modelling is an ideal trial to test the environmental processes over extensive space and  
44 time domains. In the recent decades, considerable progress has been made in pre-  
45 instrumental temperature modelling at both hemispheric and regional scales (e.g. Mitchell  
46 et al., 2005; Rutherford et al., 2005). Luterbacher et al. (2004) and Xoplaki et al. (2005)  
47 were able to map seasonally resolved temperature reconstructions across European land  
48 areas back to 1500. In particular, Luterbacher et al. (2004) developed separate multiple  
49 regression equations between each principal component (PC) of the instrumental data and  
50 all leading PC of the proxy records. In this way, they assimilated proxy records into  
51 reconstructions of the underlying spatial patterns of past climate changes. The  
52 reconstructed climate field allows for a special assessment of the spatial coherence of past  
53 annual-to-decadal temperature changes at sub-continental scale, thus providing insight  
54 into the mechanisms or forcing underlying observed variability. In hemispheric,  
55 continental and regional reconstructions, however, multi-proxy coverage is often irregular  
56 and heterogeneous (Esper et al., 2002). Temperature and precipitation reconstructions,  
57 although well developed over large geographical areas, may become poorly accurate at  
58 sub-regional and local scales, or over particular periods (Mann et al., 2000; Ogilvie and  
59 Jónsson, 2001; Diodato et al., 2008). On the other hand, it is not surprising if Mann  
60 (2007), comparing estimated regional temperatures at different locations over the past  
61 1000 years, found that the cold and warm periods were considerably different from region  
62 to region. Then, the issue of sub-regional reconstructions should attract the attention of  
63 scientists as it may exhibit unexpected results, especially regarding some temperature  
64 extremes (Bhatnagar et al., 2002). The issue of downscaling to small spatial and temporal

65 scales must be made a priority in order to achieve a better understanding of sub-regional  
66 climates (Riedwyl et al., 2009). Documentary proxies' investigation remains a reliable  
67 approach to trace back the temperature extremes before the advent of instrumental  
68 recording of meteorological data (Brázdil et al., 2005; Jones et al., 2009). Brewer et al.  
69 (2007) investigated tree-ring sites to support the reconstruction of historical droughts in  
70 Mediterranean areas during the last 500 years. However, temperature series have not been  
71 modelled for this region so far. Moreover, continuous and homogeneous instrumental  
72 series cannot be extended before the 19<sup>th</sup> century (Camuffo et al., 2010). On the other  
73 hand, high-resolution climate information is increasingly needed for the study of past, present  
74 and future climate changes (Vrac et al., 2007).

75 Several authors such as Luterbacher and Xoplaki, (2003), Pauling et al. (2003), and Ge  
76 et al. (2005) suggested that pre-modern instrumental weather indices may be promising to  
77 enrich climate reconstructions. Different sets of proxy-variables have indeed been used to  
78 find out relationships between predictors and predictands in high-resolution climate time  
79 reconstructions (e.g. Wang et al., 1991; Briffa et al., 2002; Larocque and Smith, 2005;  
80 Moberg et al., 2005; Diodato, 2007; Davi et al., 2008). Many of these reconstructions  
81 depend on empirical relationships between proxy records and climate data. Comparing  
82 linear algorithms and neural networks, Helama et al. (2009) proved that both the  
83 approaches are reliable for temperature reconstruction. Although regression-based  
84 techniques have been used with considerable success for climate reconstructions, they can  
85 engender bias in the estimates if not employed with care (Robertson et al., 1999; Moberg  
86 et al., 2005; von Storch et al., 2005). Moreover, these relationships are seldom based on a  
87 training process capable to capture all the possible data combinations that occur when  
88 extrapolation is performed (i.e. reconstruction period). With reference to  
89 dendroclimatological studies, correlation between tree-ring proxies and temperature data  
90 was found to only explain about 50% of the (Liang et al., 2008; Helama et al., 2009; Tan  
91 et al., 2009). Documentary data series are expected to better correlate with temperature,  
92 the overall explained variance being of about 70% (Leijonhufvud et al., 2008; Dobrovolný  
93 et al., 2010). However, there are few estimates of uncertainty in documentary based  
94 climate reconstructions (Moberg et al., 2009).

95 In this study, we have considered an alternative approach to address the statistical  
96 modelling of temperature variability, based on documentary records and previous large-  
97 scale reconstructions. In particular, a documentary-based technique was developed based  
98 on multiscale temperature regression (MTR)–model at sub-regional level. An area

99 covering Southern and Central Italy and named in this paper Mediterranean Sub-regional  
100 Area (MSA) is the focus of the investigation. The goal was to produce a relatively  
101 simplified multiscaled model acceptable and verifiable by scientists as well as  
102 knowledgeable people. (MTR)–model combines documentary proxy-based local weather  
103 anomalies with large-scale temperature data to adapt regional temperature data to specific  
104 sites and seasons. The selected sub-region, centrally located in the Mediterranean region,  
105 is an interesting test area rich in documentary proxy data and modern weather records  
106 useful to improve the spatial resolution of past climate. The next section describes the  
107 geographical environment, the datasets and the developed methods. Section 3 illustrates the  
108 novel mixed-model approach in detail. Its results on temperature series estimation were  
109 evaluated over the MSA. Conclusions (Section 4) point out the main results and look at  
110 horizons for future research.

111

## 112 **2 Environmental setting, data and methods**

113

### 114 **2.1 Study area, datasets and method of analysis**

115 The study is based on a set of both monthly-modelled regional temperatures and  
116 documentary proxy data at a typical Mediterranean area of Central and Southern Italy  
117 (MSA in Fig. 1). This sub-region is frequently crossed by depressions generating over the  
118 Mediterranean Sea (Wigley, 1992) that, reinforced by continental North easterly airflows,  
119 produce important fluctuations in temperature and precipitation and large-scale  
120 atmospheric oscillations (Barriendos Vallve and Martin-Vide, 1998).

121 Regional temperature data (hereafter called  $T_R$ ) were derived from Luterbacher et al.  
122 (2004) for Europe over 1500-2002. The data, upscaled at about 0.5-degree grid resolution  
123 (~50 km) from historical instrumental series and multi-proxy data  
124 (<http://www.ncdc.noaa.gov/cgi-bin/paleo/eurotemp.pl>), covers an area extending from 25°  
125 West to 40° East and from 35° to 70° North (Fig. 1a). From this map and from that  
126 depicted in Fig. 1b, it is also possible to observe the temperature-data missing over  
127 Southern Europe (including the MSA), as suggested by both data-density and correlation  
128 pattern.

129 In order to fill this deficiency in the data available, a new documentary-dataset was  
130 derived from chronicles found in two main sources, *Moio and Susanna Manuscript*  
131 (Ferrari, 1977) and *Corradi's Annals* (Corradi, 1972). A data bank (Catalogue EVA –

132 Environmental Events of the ENEA – Italian National Agency of for New Technologies,  
133 Energy and the Environment, Clemente and Margottini, 1991) was also referred to and  
134 used when necessary. The Italian scientist Alfonso Corradi (1833-1892) carried out  
135 pioneering works in documentary research on the environmental and climatological  
136 extreme conditions that occurred in Italian regions through time. He collected the  
137 historical documents from 5 to 1850 A.C., related to meteorology and epidemics into a  
138 five-volume book (Corradi, 1972). More recently, the historian Umberto Ferrari published  
139 the chronicles of Giovanni Battista Moio and Gregorio Susanna quoting climate extremes,  
140 famines from 1710 to 1769 and weather information over the 16<sup>th</sup> and 17<sup>th</sup> centuries for  
141 the Calabrian region (Ferrari, 1977).

142 For the purposes of modelling, the split-samples approach was used to segregate the  
143 available data into a calibration set and a validation set. Particular attention was paid to  
144 the calibration procedure in order to ensure that the resulting model could produce  
145 reliable outcomes (i.e. time-series reconstruction). Two distinct climate periods (1867-  
146 1903 and 1972-2002) were included in the calibration dataset (68 years in total) for two  
147 main reasons. The first was to ensure model calibration accuracy by accounting for both  
148 cold and warm intervals, and the second to ensure that the model was able to simulate air  
149 temperature on periods with either accurate (as in recent times) or inaccurate data (as in  
150 historical times). The validation dataset contained instrumental temperature  
151 reconstruction for the MSA (as performed by Camuffo et al., 2010), including the periods  
152 1742-1754 and 1792-1818. These two intervals are considered the only reliable records in  
153 the historical time for this area. The entire workflow was executed interactively using a  
154 spreadsheet of MS Excel 2003, for data collection, model development and graphical  
155 assembling, with the support of STATGRAPHICS online statistical package  
156 (<http://www.statgraphics.com>) and Statistics Library–R modules (Wessa, 2009) for  
157 statistics performance and graphical outputs, respectively. The agreement between  
158 estimates and observations was evaluated using a set of statistics, including the modelling  
159 efficiency by Nash and Sutcliffe (1970), ranging from negative infinity to positive unity  
160 (the latter being the optimum value). In order to have a visual inspection of the quality of  
161 results, a set of comparative scatterplots and histograms are also presented.

162

## 163 **2.2 Monthly temperature anomaly scaled index**

164 Information held in the written documentary sources was extracted to derive temperature  
165 related indices. Different types of indices have been proposed in historical climatology

166 studies (Pfister, 1999, 2001; Brázdil et al, 2005). As a general reference, a seven-point  
167 scale was employed, ranging from -3 for 'extreme coldness' to +3 for 'extreme hotness',  
168 with 0 indicating 'normal' conditions. However, this ordinal scale bears the limitation of a  
169 limited discrimination across the full range of extremes, since it tends to assign all events  
170 above a certain level to the same extreme class (Glaser and Riemann, 2009). To obtain a  
171 more realistic degree of variability in the temperature modelling, we used a simplified  
172 scaled-index for a more accurate estimate of extreme anomalies. Examples of such events  
173 are recorded only during the Little Ice Age (e.g. rivers freezing), when no instrumental  
174 data could overlap the calibration period.

175 Based on the above criteria, monthly indices were calculated, thus gaining more than  
176 seven possible classes to preserve the variability described by the written sources similar  
177 to the natural variability, and over a longer period than the calibration interval. These  
178 classes were allocated to their respective index by an asymmetric look-up table in order to  
179 take into account temporal shifts between proxy and actual anomalies in different seasons  
180 of the year. In fact, as an example, a river freezing on March or April is a more negative  
181 anomaly than a frozen river on January. Based on these new classification principles,  
182 temperature anomalies were coded for winter and summer by means of a monthly-based  
183 Temperature Anomaly Scaled Index (*TASI*), according to the look-up table scheme (Table  
184 1a). The geometric interpretation of the classification process is shown in Fig. 2. The  
185 asymmetric profile for winter and summer seasons is a bi-dimensional simplification based  
186 on observations and documentary-proxy data. For the study-area, positive (red line) and  
187 negative (blue line) temperature anomalies result asymmetrically arranged around the mean  
188 seasonal values (black line). The latter are long-term average temperatures calculated, for  
189 the study-area, from the European database of Luterbacher et al. (2004). In the case of  
190 negative anomalies, the baseline is the freezing point of water (0 °C). A baseline for all  
191 seasons was not set to reproduce positive anomalies. In this case, in fact, temperature  
192 extremes are dictated by the Mediterranean latitudes. Although this region presents a  
193 twofold climate regime, where both tropical and mid-latitude aspects play a role, the  
194 latitudinal radiative flux stands out as the main factor determining the temperature.  
195 Advective transport off northern Africa can also occasionally affect the Mediterranean, but  
196 the seasonal variations are well marked (e.g. Schiano et al., 2000; Lionello et al., 2006) and,  
197 notably, temperatures in winter are never as high as summer values. Negative anomalies  
198 were assigned to cover the gap between the mean value and the freezing point, which is  
199 only sporadically (or never) approached in summertime (N/A). In winter (December,

200 January, and February), values of -1 (cold) / +1 (warm) and -2 (very cold) / +2 (very  
201 warm) are consistent with temperature values deviating up to three and four times the  
202 standard deviation, respectively. Abrupt jumps from “very cold” (-2) to “freezing” (-4) in  
203 winter are due to the lack of appreciative intermediate states during the calibration period.  
204 In the case of positive anomalies, a similar scheme is reproduced for summer season  
205 (June, July and August). Negative anomalies are instead doubled (July-August) or tripled  
206 (June) compared to winter, because most evidence of “cold” and “very cold” conditions  
207 in the historical sources only refers to cooling to temperatures well below the seasonal  
208 mean.

209 Once the magnitude of the indices array was defined, then the proxies were  
210 transformed into a time series with a clearly defined temporal resolution. This kind of  
211 understanding is offered in the form of an exemplary table layout (Table 1b),  
212 incorporating monthly and seasonal values of the *TASI*, and the relative sources for the  
213 period 1752-1757.

214

### 215 **3 Modelling of sub-regional winter temperatures**

216

217 In this study, regional temperatures (*case*) from Luterbacher et al. (2004) are the basis for  
218 modelling sub-regional temperatures (*response*). In this situation, it is possible to have  
219 more than one response for each case. Thus, a central problem in the analysis of  
220 multiresponse situations, is finding a function that combines several responses to  
221 determine more realistic estimates. This is also the case of air temperature, for which  
222 multi-scale predictors are needed to model over different space- and time-domains (after  
223 Bates and Watts, 2007). In this way, the information collected (regional temperature data)  
224 was downscaled to reasonably approximate the behaviour of the disturbance terms (or  
225 stimulus variables) driving the temperature measurements at sub-regional scale. These  
226 approximations reside on the general assumption that sub-regional air temperature  
227 depends on two disturbance terms: regional-synoptic forcing and local weather  
228 conditions. The regional scale can drive the general temperature trend, while area-specific  
229 temperatures are met by local conditions. Weather variables and climate indices were  
230 both used as predictors as basis of the multi-scale regression model.

231

#### 232 **3.1 Inferences for multi-scale temperature estimation**

233 A statistical model of sub-regional temperature estimation was created with aims of  
234 prediction and explanation. For prediction, the model structure was generated based on



235 Box and Draper (1972). In particular, a determinant parameter-estimation criterion for  
 236 multiresponse data was derived upon the primary assumption that the disturbance terms  
 237 of different cases are uncorrelated. A corollary assumption was that, in a single case, the  
 238 disturbance terms have a fixed, unknown variance-covariance matrix for different  
 239 responses. A model was written along this path, assuming multiple responses and  
 240 dependence on a set of parameters, as referred to by Bates and Watts (2007): the  
 241 temperature random variable is a function depending on some predictors by a set of  
 242 parameters, and assuming the sum of the errors equal to zero.

243 To contribute to the aim of explanation, influential predictors were identified and  
 244 insight gained into the relationship between the predictors and the outcome based on  
 245 climate history and modelling background. In this path, the temperature random variable  
 246 comprises predicting variables at regional, ( $\cdot$ )<sub>R</sub>, and sub-regional, ( $\cdot$ )<sub>SR</sub>, scales (Fig. 3).  
 247 Once regional and sub-regional components are identified, one can estimate the  
 248 relationship between expected temperature and predictors. To extend the procedure for  
 249 extrapolations outside the range represented by the calibration sample, the model was  
 250 iteratively rearranged towards a robust solution whereby two additive components are  
 251 used (non-linear regional component, linear-and-local component):

252

$$253 \quad y(T_{MTR}) = k \cdot \sqrt{T_R} + \beta \cdot (T_R + \Omega_S + \sum TASI_S) \quad (1)$$

254

255 where the first term,  $y(T_{MTR})$ , is the seasonal mean temperature output ( $^{\circ}\text{C}$ ) of the (MTR)–  
 256 model;  $T_R$  is the regional component of temperature ( $^{\circ}\text{C}$ ) supplied as a boundary  
 257 condition; the part in brackets is the sub-regional component of temperature ( $^{\circ}\text{C}$ ) supplied  
 258 as a local constraint.

259 A recursive procedure was performed in order to obtain the best fit of a regression  
 260 equation  $Y=a+b \cdot X$ , where  $Y$ =model estimates and  $X$ =actual data, according to the  
 261 following criteria:

262

$$263 \quad \begin{cases} a = 0 \\ |b - 1| = \min \\ R^2 = \max \end{cases} \quad (2)$$

264

265 where the first condition is to set null intercept ( $a$ ), the second is to approximate the unit  
 266 slope ( $b$ ) of the straight line that would minimize the bias, and the third is to maximize the  
 267 goodness-of-fit ( $R^2$ ) of the linear function. Since the different assumptions cannot be

268 guaranteed *a priori*, the parameters were estimated using an iterative, knowledge-driven  
269 approach to bias correction steps (after Box et al., 1978). For instance, after a first run, it  
270 was found that regional temperatures ( $T_R$ ) introduced increasingly biased and imprecise  
271 estimates over historical times. Likewise, earliest regional inferences in Mann et al.  
272 (2000) tended to be associated with decreased performance. To account for this non-  
273 invariance over the historical time-scale, a power law was assigned to  $T_R$  with the  
274 exponent forced to be lower than one (and finally set equal to 0.5) to rebalance internally  
275 the quality of calibration. Such iterative fitting of the data allowed for correcting the bias  
276 initially observed and capturing the full range of sub-regional scale variability.  
277 The scale parameter  $k$  ( $^{\circ}\text{C}^2$ ) was initially set equal to one and, for reasons of parsimony as  
278 by Grace (2004), not treated as a free parameter because the initial value resulted in a fit  
279 that satisfied the criteria outlined above (Eq. 2).  $T_R$  appears in both the square root (power  
280 of 0.5) and linear term. In the first case, it returns a direct, non-linear effect, while in the  
281 brackets it crosses the sub-regional anomalies identified by the *TASI* to correct the bias  
282 observed in the historical times. The square root of  $T_R$  and parameter  $\beta$  are mainly to  
283 define the order of magnitude of the process used to downscale the (MTR)–model to the  
284 sub-regional scale. The other two terms into the brackets are seasonally-varying (index  $S$ )  
285 shift parameters ( $^{\circ}\text{C}$ ) of  $T_R$ , which force the model with meteorological ( $\Sigma TASI_S$ , sum of  
286 monthly values of the Temperature Anomaly Scaled Index defined above) and  
287 climatological ( $\Omega_S$ , hereafter indicated as  $\Omega_w$  and  $\Omega_s$  for winter and summer, respectively)  
288 boundary conditions.

289

### 290 **3.2 Model parameterization and evaluation**

291 For (MTR)–model (Eq. 1), the values of the parameters obtained from a particular set of  
292 observations with a recursive procedure are:  $\beta=0.268$ ,  $\Omega_w=11.0$   $^{\circ}\text{C}$ ,  $\Omega_s=43.5$   $^{\circ}\text{C}$ . Using the  
293 estimated parameter values, the non-linear response to  $T_R$  is depicted in Fig. 3, as  
294 translated into Eq. 1 for different values of  $\Sigma TASI_S$ .

295 In the temperature series supplied by Luterbacher *et al.* (2004), standard deviation (sd)  
296 for winter increases in more recent years, i.e. after the LIA (sd=0.96 against 0.74 for  
297 1739-1783). This contrasts with the instrumental observations, for instance those  
298 performed by Domenico Cirillo in the 18<sup>th</sup> century (sd=1.1) and documented by the  
299 Meteorological Diaries of the Royal Society of London for the Kingdom of Naples  
300 (Derham, 1733-1734). The reconstructed series based on Eq. (1) gives sd~1.0 for both

301 recent and historical times. For summertime,  $sd \sim 0.6$  was registered for 1739-1783 in the  
302 regional dataset, also approached by the reconstructed series.

303 The parameter values estimated from the data roughly matched the observations. In  
304 Fig. 4, negligible departures of the data-points from the 1:1 line (observed versus  
305 predicted values) indicate the presence of limited bias in the residuals with both winter  
306 (graph a) and summer (graph b) calibration datasets. The Nash-Sutcliffe efficiency index  
307 and the correlation coefficient, equal to 0.88 and 0.94 for winter and 0.87 and 0.88 for  
308 summer (Table 2), are also satisfactory. Fig. 5 shows the results of model validation  
309 against independent time-series data. In general, fluctuations of observed and (MTR)–  
310 model predicted temperatures compare well in both seasons. In particular, absolute  
311 minimum and maximum observed values are both reflected in the predictions (black lines  
312 in Fig. 5a, b). The Nash-Sutcliffe efficiency values, equal to 0.66 (winter) and 0.63  
313 (summer) are also satisfactory (Table 2). In contrast, the regional model by Luterbacher et  
314 al. (2004) poorly reflects the variability of actual winter temperature in both seasons  
315 (circles in Fig. 5a), as also confirmed by the correlation coefficient and the Nash-Sutcliffe  
316 efficiency values (equal to 0.26 and  $-0.43$ , for winter, and 0.50 and  $-0.30$  for summer,  
317 Table 2, validation dataset). In wintertime, regional estimates suffer from reduced  
318 precision in Southern Europe where temperatures are more variable than Central Europe.  
319 In summertime, when estimated and observed variances are similar, most assessments of  
320 the poor performance of regional estimates focus on the weak correlation with  
321 observations (Fig. 1b). For (MTR)–model, the residuals distribution denote a quasi-  
322 Gaussian trend (Fig. 6a, b), with the QQ-plots reflecting theoretical values (Fig. 6a<sub>1</sub>, b<sub>1</sub>) in  
323 both seasons.

324 Independence-of-errors due to the possible presence of significant autocorrelations  
325 among the residuals was also tested. Strong temporal dependence may in fact induce  
326 spurious relations according to standard inference in an ordinary regression model (see  
327 Granger et al., 2001), and the same problem is further increased in the context of  
328 nonlinear models (Stenseth et al., 2003). The Durbin-Watson (Durbin and Watson, 1950,  
329 1951)  $d$  statistic in the following form was calculated to verify the presence of  
330 autocorrelation in the residuals  $e$  (the index  $t$  indicating the  $t^{\text{th}}$  year):

331

$$d = \frac{\sum_{t=1}^T (e_t - e_{t-1})^2}{\sum_{t=1}^T e_t^2} \quad (3)$$

333

334 Two critical values,  $d_{L,\alpha}$  and  $d_{U,\alpha}$ , vary depending on the level of significance ( $\alpha$ ), the  
 335 number of observations, and the number of predictors in the regression equation. In the  
 336 calibration dataset, indication of possible correlation is produced at  $0.01 < \alpha < 0.05$   
 337 significance level for winter only (Table 2). The existence of the autocorrelation can be  
 338 understood as the result of a functional misspecification problem (e.g. Green, 2003). This  
 339 aspect is similar to the multicollinearity problem in linear regression, usually dealt with  
 340 separately from autocorrelation, but also examined by its autocorrelation effect in the  
 341 error term (e.g. Ramsey III et al., 2001). In our case, autocorrelation may be due to some  
 342 internal constraint in the calibration stage, probably related to the fact that winter  
 343 temperatures in the regional dataset and model outputs are more similar in recent times  
 344 (the period of years used for calibration) than it was in historical times. The calibration  
 345 dataset is from recent times (covering periods around the 20<sup>th</sup> century), when estimates  
 346 from Luterbacher et al. (2004) better approach observed temperatures. Under such  
 347 conditions, the model likely represents some redundancy in the explanatory variables that  
 348 means, other predictors than the regional temperature component might not be effective in  
 349 improving upon the sub-regional estimates. However, both calibration results in summer  
 350 and the results of data validation in both seasons assume statistical independence of the  
 351 residuals, with type-I error probability of 0.09 and 0.36 of Durbin-Watson test statistic  
 352 (Table 2).

353 The mean absolute error (0.24-0.33), similar between calibration and validation and  
 354 between seasons, and the other statistics of Table 2 indicate for the validation set a  
 355 satisfactory performance. This suggests that the proposed approach is a promising tool for  
 356 future applications in temperature estimation.

357 The scope of our modelling approach and model parameterization was restricted to  
 358 capturing the temporal variability of seasonal temperature data in the study-area, and  
 359 some limitations of the methodology should be acknowledged. Uncertainty ranges in the  
 360 estimation of parameters were not formally accounted because parameter estimation was  
 361 achieved in more steps, which makes confidence bounds for model parameters not easily  
 362 quantifiable. The model error (mismatch between the observed and the modelled value) is

363 however an indication of total model uncertainty (e.g. Shrestha and Solomatine, 2008),  
364 and Nash-Sutcliffe efficiency values of 0.6 can discriminate between bad and good  
365 performances (e.g. Lim et al., 2006). The efficiency values obtained in the validation  
366 stage ( $>0.8$ ) thus indicate limited model uncertainty; likely associated with narrow  
367 parameter uncertainty. Since the results of model calibration were satisfactory, the  
368 robustness of the solution was relied on and sensitivity analysis was not added to the  
369 study. The reconstruction of temperatures series has thus used generic optimized  
370 parameters, which are crude estimates over multiple years. This ensures a generic  
371 representation for the MSA, with evidence of improved performance compared to  
372 previous estimates. Since geographical locations have characteristics that require specific  
373 model structures and local optimization, then the application of the model to other sub-  
374 regions may be limited by the ability to provide representative drivers and parameter  
375 values.

376

#### 377 **4 Conclusions**

378

379 The main novelty of this paper is the introduction of a relatively simple model to  
380 reconstruct past seasonal (winter and summer) temperature variability at sub-regional  
381 scale based on proxy and simulated datasets. In general, the use of data deriving from  
382 different spotted sources is not straightforward to reconstruct climate in Southern Europe.  
383 Data used in the previous seasonal temperature reconstruction over Europe, especially  
384 over the Mediterranean areas, are from few and early instrumental series (data before  
385 1850) that, for their nature, are difficult to find, evaluate, correct and convert or present in  
386 a Celsius scale in terms of temperature anomalies.

387 The multi-scale regression approached here overcomes the inherent loss of variance in  
388 both early instrumental records and univariate least-squares calibration equations. In  
389 general, multi-scale, process-based climate models can be accurate. However, the authors  
390 argue that improvements in model sophistication may not be as profitable as the ability to  
391 reconstruct confidently the overall picture of temperature-related events (and therefore  
392 temperature data) over historical times and in different geographical places. Validation,  
393 from this point of view, is a major statistical instrument to develop a reliable model to add  
394 robustness to past temperature reconstructions. Furthermore, in this paper, we took  
395 advantage of the (MTR)-model versatility to evaluate, through proxy-documentary data,  
396 how the sub-regional temperatures signal is driven by local and boundary conditions. The

397 accuracy of these signals depends not only on the intrinsic properties of the model itself,  
398 but also from the possibility to recover homogeneous documentary records able to  
399 maintain unchanged the climate information and to replicate, through the model  
400 application, the actual temperature series. Once such conditions are satisfied, the  
401 modelling approach may potentially be suitable for applications elsewhere in the  
402 Mediterranean basin, provided that model parameters will be documented for other sub-  
403 regions than the one investigated here. Further research extending the modelling approach  
404 developed here towards other sub-regions of the Mediterranean area would provide  
405 additional insight into the implications for the production of valuable knowledge from  
406 proxy documentary data and can be considered the natural evolution of this study.

407

## 408 **References**

409

- 410 Barriendos Vallve, M., and Martin-Vide, J.: Secular climatic oscillations as indicated by  
411 catastrophic floods in the Spanish Mediterranean coastal area (14<sup>th</sup>-19<sup>th</sup> centuries),  
412 *Climatic Change*, 38, 473-491, 1998.
- 413 Bates, D.M., and Watts D.G. (Eds.): *Nonlinear regression analysis and its applications*,  
414 John Wiley & Sons, Little Falls, NJ, USA, 2007.
- 415 Bhatnagar, A., Jain, K., and Tripathy, S.C.: Variation of solar irradiance and mode  
416 frequencies during Maunder minimum, *Astrophys.Space Sci.*, 281, 761–764, 2002.
- 417 Box, M.J., and Draper, N.R. (Eds.): *Estimation and design criteria for multiresponse*  
418 *nonlinear models with non-homogeneous variance*, *Applied Statistics*, 21, 13-24, 1972.
- 419 Box, G.E.P., Hunter, W.G., and Hunter, J.S.: *Statistics for experimenters: an introduction*,  
420 John Wiley and Sons, New York, NY, USA, 1978.
- 421 Brázdil, R., Pfister, C., Wanner, H., von Storch, H., and Luterbacher, J.: Historical  
422 climatology in Europe – The state of the art, *Climatic Change*, 70, 363-430, 2005.
- 423 Brewer, S., Alleaume, S., Guiot, J., and Nicault, A.: Historical droughts in Mediterranean  
424 regions during the last 500 years: a data/model approach, *Clim. Past*, 3, 355-366, 2007.
- 425 Briffa, K.R., Osborn, T.J., Schweingruber, F.H., Jones, P.D., Shiyatov, S.G., and  
426 Vaganov, E.A.: Tree-ring width and density data around the Northern Hemisphere:  
427 Part 1, local and regional climate signals, *Holocene* 12, 737–757, 2002.
- 428 Camuffo D., Bertolin, C., Barriendos, M., Dominguez-Castro, F., Cocheo, C., Enzi, S.,  
429 Sghedoni, M., della Valle, A., Garnier, E., Alcoforado, M.J., Xoplaki, E., Luterbacher,

430 J., Diodato, N., Maugeri, M., Nunes, M.F., and Rodriguez, R.: 500-year temperature  
431 reconstruction in the Mediterranean Basin by means of documentary data and  
432 instrumental observations, *Climatic Change*, 101, 169-199, 2010.

433 Camuffo, D., and Enzi, S.: Reconstructing the climate of northern Italy from archive  
434 sources, in: *Climate since A.D. 1500*, Routledge, London, United Kingdom, 143-154,  
435 1992.

436 Clemente, G.F., and Margottini, C.: Sistema EVA: una biblioteca di dischi ottici per le  
437 catastrofi naturali del passato, *Prometeo*, 9, 22-29, 1991 (in Italian).

438 Corradi, A.: Corradi Alfonso: *Annali delle epidemie occorse in Italia dalle prime*  
439 *memorie fino al 1850*, five volumes, Società medico-chirurgica di Bologna (Ed.),  
440 Forni, Bologna, Italy, 1972 (in Italian).

441 Davi, N.K., Jacoby, G.C., D'Arrigo, R.D., Baatarbileg, N., Jinbao, L., and Curtis, A.E.: A  
442 tree-ring-based drought index reconstruction for far-western Mongolia: 1565-2004, *Int.*  
443 *J. Climatol.*, 29, 1508-1514, 2008.

444 Derham, W. 1733-1734. An abstract of the Meteorological Diaries, communicated to the  
445 Royal Society, with re-marks upon them, by W. Derham, D. D. Canon of Windsor, F.  
446 R. S. [Vide Part III. In *Transact. No 433.*] Part IV. *Philosophical Transactions (1683-*  
447 *1775)*, 38, 405-412.

448 Diodato N.: Climatic fluctuations in Southern Italy since 17<sup>th</sup> century: reconstruction  
449 with precipitation records at Benevento, *Climatic Change*, 80, 411-431, 2007.

450 Diodato, N., Ceccarelli, M., and Bellocchi, G.: Decadal and century-long changes in the  
451 reconstruction of erosive rainfall anomalies at a Mediterranean fluvial basin, *Earth*  
452 *Surf. Proc. Land*, 33, 2078–2093, 2008.

453 Dobrovolný, P., Moberg, A., Brázdil, R., Pfister, C., Glaser, R., Wilson, R., van Engelen,  
454 A., Limanówka, D., Kiss, A., Halíčková, M., Macková, J., Riemann, D., Luterbacher,  
455 J., and Böhm, R.: Monthly, seasonal and annual temperature reconstructions for  
456 Central Europe derived from documentary evidence and instrumental records since AD  
457 1500, *Climatic Change* 101, 69-107, 2010.

458 Durbin, J., and Watson, G.S.: Testing for serial correlation in least squares regression, I,  
459 *Biometrika* 37, 409-428, 1950.

460 Durbin, J., and Watson, G.S.: Testing for serial correlation in least squares regression, II,  
461 *Biometrika* 38, 159-179, 1951.

462 Esper, J., Cook, E.R., and Schweingruber, F.H.: Low frequency signals in long tree-ring  
463 chronologies for reconstructing past temperature variability, *Science*, 295, 2250-2253,  
464 2002.

465 Ferrari, U. (Ed.): Giovan Battista Moio, Gregorio Susanna: Diario di quanto successe in  
466 Catanzaro dal 1710 al 1769, Edizioni Effe Emme, Chiaravalle Centrale, 1977 (in Italian).

467 García-Herrera, R., Luterbacher, J., Lionello, P., González-Rouco, F., Ribera, P., Rodó,  
468 X., Kull, P., and Zerefos, C.: Reconstruction of past Mediterranean climate, *Eos*  
469 *Transaction of the American Geophysical Union*, 88, doi:10.1029/2007EO090010,  
470 2007.

471 Ge, Q-S, Zheng, J-Y, Hao, Z-X, Zhang, P-Y, and Wang, WC.: Reconstruction of  
472 historical climate in China: high-resolution precipitation data from Qing Dynasty  
473 Archives, *B. Am. Meteorol. Soc.*, 86, 671-679, 2005.

474 Glaser, R., and Riemann, D.: A thousand-year record of temperature variations for  
475 Germany and Central Europe based on documentary data, *J. Quaternary Sci.*, 24, 437-  
476 449, 2009.

477 Grace, R.C.: Temporal context in concurrent chains : I. Terminal-link duration, *Journal of*  
478 *the Experimental Analysis of Behaviour*, 81, 215-237.

479 Granger, C.W.J., Hyung, N., and Jeon, Y.: Spurious regressions with stationary series,  
480 *Applied Economics*, 33, 899–904, 2001.

481 Green, W.: *Econometric analysis*, New York University, 5<sup>th</sup> Edition, Prentice Hall, New  
482 York, 2003.

483 Helama, S., Makarenko, N.G., Karimova, L.M., Kruglun, O.A., Timonen, M.,  
484 Holopainen, J. Meriläinen, J., and Eronen, M.: Dendroclimatic transfer functions  
485 revisited: Little Ice Age and Medieval Warm Period summer temperatures  
486 reconstructed using artificial neural networks and linear algorithms, *Annales*  
487 *Geophysicae*, 27, 1097–1111, 2009.

488 Jones, P.D., Briffa, K.R., Osborn, T.J., Lough, J.M., van Ommen, T.D., Vinther, B.M.,  
489 Luterbacher, J., Wahl, E.R., Zwiers, F.W., Mann, M.E., Schmidt, G.A., Ammann,  
490 C.M., Buckley, B.M., Cobb, K.M., Esper, J., Goosse, H., Graham, N., Jansen, E.,  
491 Kiefer, T., Kull, C., Küttel, M., Mosley-Thompson, E., Overpeck, J.T., Riedwyl, N.,  
492 Schulz, M., Tudhope, A.W., Villalba, R., Wanner, H., Wolff, E., and Xoplaki, E.:  
493 High-resolution palaeoclimatology of the last millennium: a review of current status  
494 and future prospects, *Holocene* 19, 3-49, 2009.



495 Larocque, S.J., and Smith, D.J.: A dendroclimatological reconstruction of climate since  
496 AD 1700 in the Mt. Waddington area, British Columbia Coast Mountains, Canada,  
497 *Dendrochronologia* 22 , 93-106, 2005.

498 Leijonhufvud, L., Wilson, R., and Moberg, A.: Documentary data provide evidence of  
499 Stockholm average winter to spring temperatures in the eighteenth and nineteenth  
500 centuries, *Holocene*, 18, 333-343, 2008.

501 Liang, E., Shao, X., and Qin, N.: Tree-ring based summer temperature reconstruction for  
502 the source region of the Yangtze River on the Tibetan Plateau, *Global Planet. Change*,  
503 61, 313-320, 2008.

504 Lim, K.J., Engel, B.A., Zang, T., Muthukrishnan, S., Choi, J., and Kim, K.: Effects of  
505 calibration on L-THIA GIS runoff and pollutant estimation, *J. Environ. Manage.*, 78,  
506 35-43, 2006.

507 Lionello, P., Malanotte-Rizzoli, P., and Boscolo, R.: *Mediterranean climate variability,*  
508 *Developments in Earth and Environmental Sciences, Vol. 4, Elsevier, Amsterdam,*  
509 2006.

510 Luterbacher, J., Dietrich, D., Xoplaki, E., Grosjean, M., and Wanner, H.: European  
511 seasonal and annual temperature variability, trends and extremes since 1500, *Science*,  
512 303, 1499-1503, 2004.

513 Luterbacher, J. and Xoplaki, E.: 500-year winter temperature and precipitation variability  
514 over the Mediterranean area and its connection to the large-scale atmospheric  
515 circulation, in: *Mediterranean climate variability and trends*, Springer-Verlag, Berlin,  
516 Germany, 133-153, 2003.

517 Mann, M.E.: Climate over the past two millennia, *Annual Rev. Earth Pl. Sc.*, 35, 111-136,  
518 2007.

519 Mann, M.E., Gille, E., Bradley, R.S., Hughes, M.K., Overpeck, J., Keimig, F.T., and  
520 Gross, W.: Global temperature patterns in past centuries: an interactive presentation,  
521 *Earth Interact.*, 4, 1-29, 2000.

522 Mitchell, T., and Jones, P.D., An improved method of constructing a database of monthly  
523 climate observations and associated high-resolution grids, *Int. J. Climatol.*, 25, 693–  
524 712, 2005.

525 Moberg, A., Dobrovolny, P., Wilson, R., Brázdil, R., Pfister, C., Glaser, R.,  
526 Leijonhufvud, L., and Zorita, E.: Quantifying uncertainty in documentary-data based  
527 climate reconstructions?, *Geophysical Research Abstracts*, 11, EGU2009-1177, 2009.

Mis en forme : Anglais  
(Royaume-Uni)

528 Moberg, A., Sonechkin, D.M., Holmgren, K., Datsenko, N.M., and Karlén, W.: Highly  
529 variable Northern Hemisphere temperatures reconstructed from low- and high-  
530 resolution proxy data, *Nature*, 433, 613–617, 2005.

531 Nash, J.E., and Sutcliffe, J.V.: River flow forecasting through conceptual models part I -  
532 A discussion of principles, *J. Hydrol.*, 10, 282–290, 1970.

533 Ogilvie, A.E.J., and Jonsson, T.: Little Ice Age research: a perspective from Iceland,  
534 *Climatic Change*, 48, 9-52, 2001.

535 Pauling, A, Luterbacher, J, and Wanner, H.: Evaluation of proxies for European and  
536 North Atlantic temperature field reconstructions, *Geophys. Res. Lett.*, 30, 1787,  
537 doi:10.1029/2003GL017589, 2003.

538 Pfister, C.: *Wetternachhersage. 500 Jahre Klimavariationen und Naturkatastrophen (1496-*  
539 *1995)*, Haupt, Bern, Switzerland, 1999 (in German).

540 Pfister, C.: I cambiamenti climatici nella storia dell'Europa. Sviluppi e potenzialità della  
541 climatologia storica, in: *Che tempo faceva. Variazioni del clima e conseguenze sul*  
542 *popolamento umano. Fonti, Metodologie e Prospettive*, Angeli, Milan, Italy, 19-60, 2001  
543 (in Italian).

544 Ramsey, E.W., III, Hodgson, M.E., Sapkota, S.K., and Nelson, G.A.: Forest impact estimated  
545 with NOAA AVHRR and Landsat TM data related to an empirical hurricane wind-field  
546 distribution. *Remote Sens. Environ.*, 77, 279-292, 2001.

547 Riedwyl, N., Küttel, M., Luterbacher, J., and Wanner, H.: Comparison of climate field  
548 reconstruction techniques: application to Europe, *Clim. Dynam.*, 32, 381-395, 2009.

549 Robertson, I., Lucy, D., Baxter, L., Pollard, A.M., Aykroyd, R.G., Barker, A.C., Carter,  
550 A.H.C., Switsur, V.R., and Waterhouse, J.S.: A kernel-based Bayesian approach to  
551 climatic reconstruction, *Holocene*, 9, 495–500, 1999.

552 Rutherford, S., Mann, M.E., Osborn, T.J., Bradley, R.S., Briffa, K.R., Highes, M.K., and  
553 Jones, P.D.: Proxy-based northern hemisphere surface temperature reconstructions:  
554 sensitivity to method, predictor network, target season, and target domain, *J. Climate*,  
555 18, 2308-2329, 2005.

556 Schiano, M.E., Borghini, M., Castellari, S., and Luttazzi, C.: Climatic features of the  
557 Mediterranean Sea detected by the analysis of the longwave radiative bulk formulae,  
558 *Ann. Geophysicae*, 18, 1482-1487, 2000.

559 Shrestha, D.L., and Solomatine, D.P.: Data-driven approaches for estimating uncertainty  
560 in rainfall-runoff modelling, *International Journal of River Basin Management*, 6, 109-  
561 122, 2008.

Mis en forme : Italien (Italie)

562 Stenseth, N.C., Ottersen, G., Hurrell, J.W., Mysterud, A., Lima, M., Chan, K.-S., Yoccoz,  
563 N.G., and Ådlandsvik, B.: Studying climate effects on ecology through the use of  
564 climate indices: the North Atlantic Oscillation, El Niño Southern Oscillation and  
565 beyond, *P. Roy. Soc. B-Biol. Sci.*, 270, 2087-2096, 2003.

566 Tan, M., Shao, X., Liu, J., and Cai, B.: Comparative analysis between a proxy-based  
567 climate reconstruction and GCM-based simulation of temperatures over the last  
568 millennium in China, *J. Quaternary Sci.*, 24, 547–551, 2009.

569 Von Storch, H., Zorita, E., Jones, J., Dimitrev, Y., Gonzalez-Rouco, F., and Tett, S.:  
570 Reconstructing past climate from noisy data, *Science*, 306, 679-682, 2005.

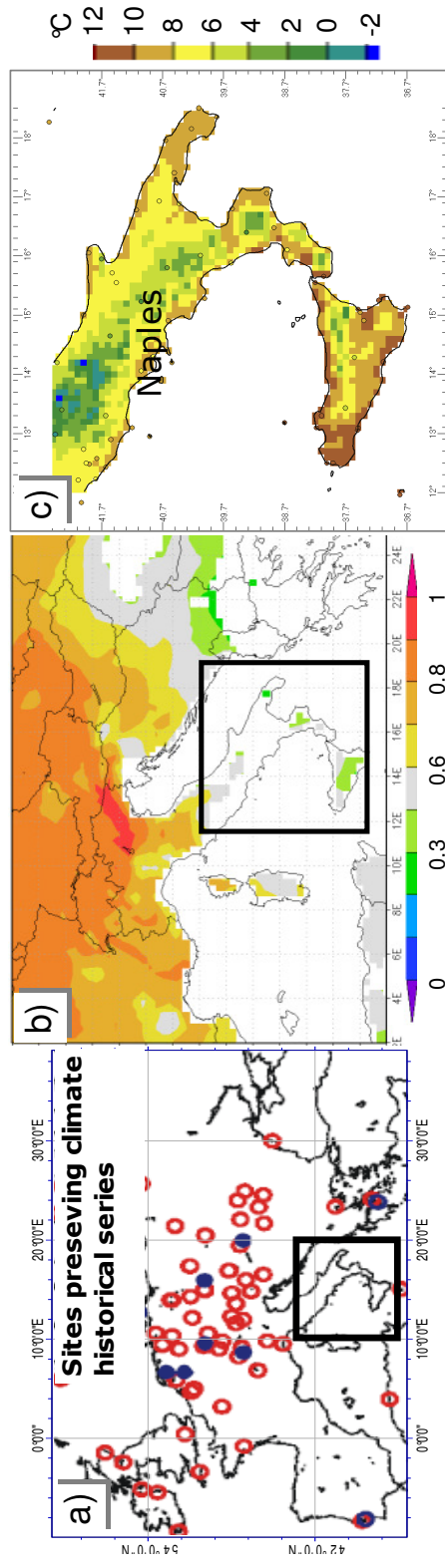
571 Vrac, M., Marbaix, P., Paillard, D., Caveau, P.: Non-linear statistical downscaling of present  
572 and LGM precipitation and temperatures over Europe, *Clim. Past*, 3, 669–682, 2007.

573 Xoplaki, E., Luterbacher, J., Paeth, H., Dietrich, D., Steiner, N., Grosjean, M., and  
574 Wanner, H.: European spring and autumn temperature variability and change of  
575 extremes over the last half millennium, *Geophys. Res. Lett.*, 32, L15713,  
576 doi:10.1029/2005GL023424, 2005.

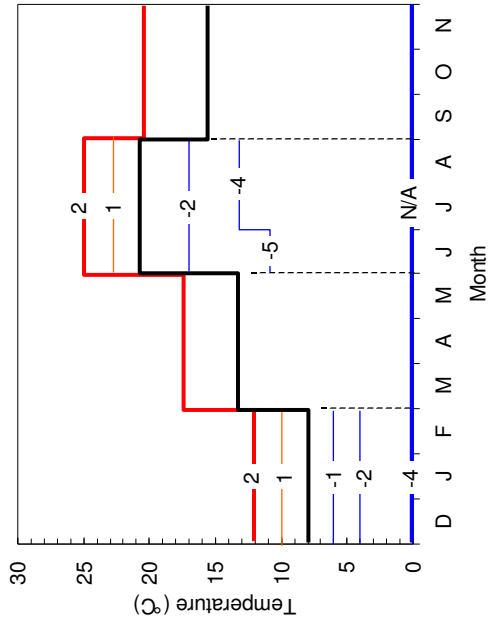
577 Wang, R., Wang, S., and Fraedrich, K.: An approach to reconstruction of temperature on  
578 a seasonal basis using historical documents from China, *Int. J. Climatol.*, 11, 381-392,  
579 1991.

580 Wessa P.: A framework for statistical software development, maintenance, and publishing  
581 within an open-access business model, *Computational Stat.*, 24, 183-193, 2009.

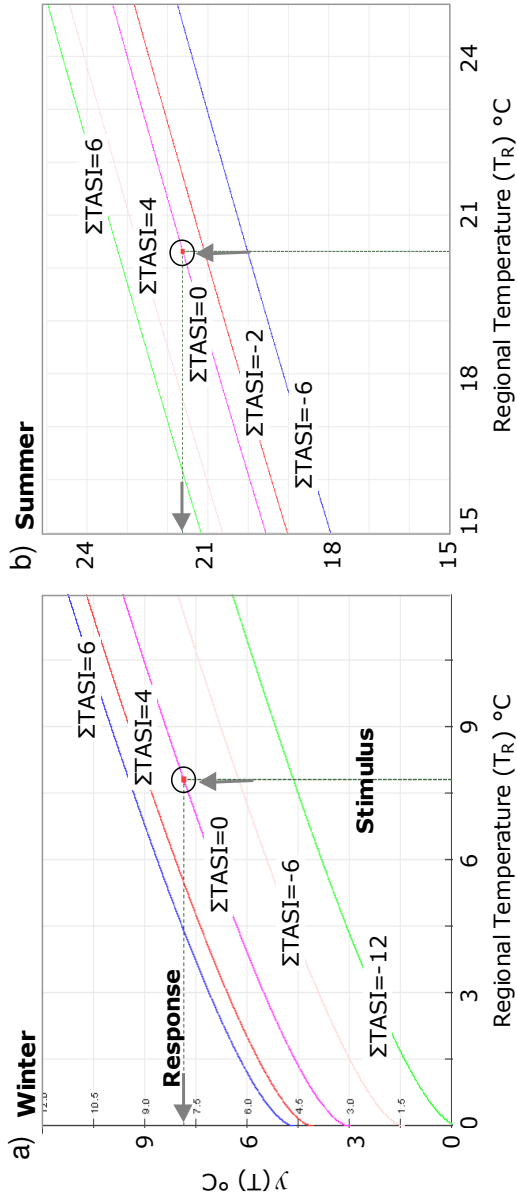
582 Wigley, T.M.L.: Future climate of the Mediterranean Basin with particular emphasis in  
583 changes in precipitation, in: *Climate change in the Mediterranean*, Edward Arnold,  
584 London, United Kingdom, 15-44.



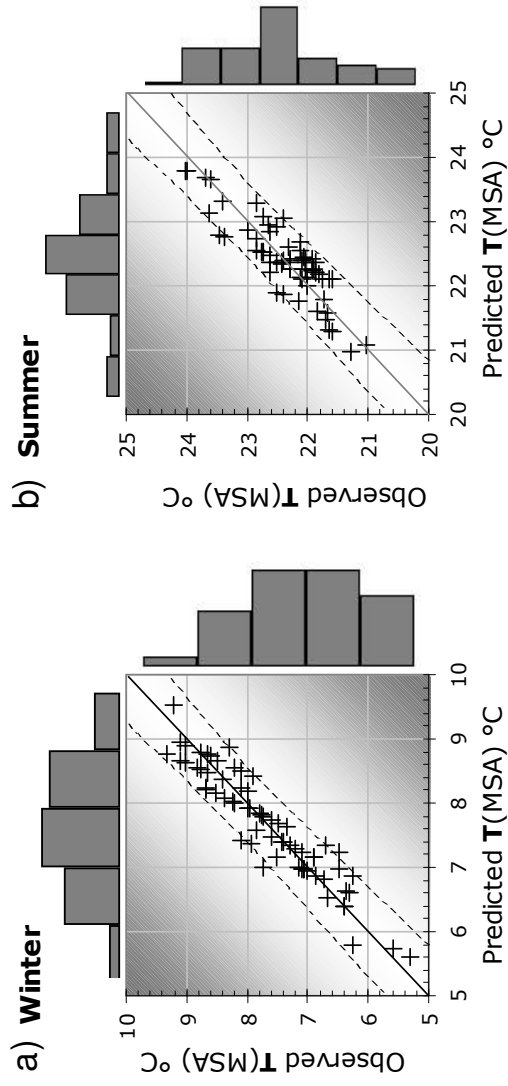
585 **Fig. 1. a):** Geographical setting of the Mediterranean Sub-regional Area (MSA, squared) with the location of temperature sites (red circles), and  
 586 documentary monthly-resolved data (blue dots) used by Luterbacher et al. (2004) to reconstruct the regional seasonal temperatures over Europe  
 587 since 1500 AD; **b):** Winter temperature correlation patterns (values rendered in white are not significant,  $p > 0.05$ ) between one grid-point of Northern  
 588 Italy (46° North, 12° East) and grid-points over central Mediterranean Europe (the MSA is squared), as processing by Climate Explorer with E-OBS  
 589 version 3.0 gridded dataset (<http://eca.knmi.nl/download/ensembles/ensembles.php>) for the period 1950-2010; **c):** Winter temperature pattern averaged  
 590 over 1961-1990 in the MSA, as arranged by LocClim FAO software at 10-km resolution ([http://www.fao.org/scd/2002/EN1203a\\_en.htm](http://www.fao.org/scd/2002/EN1203a_en.htm)).



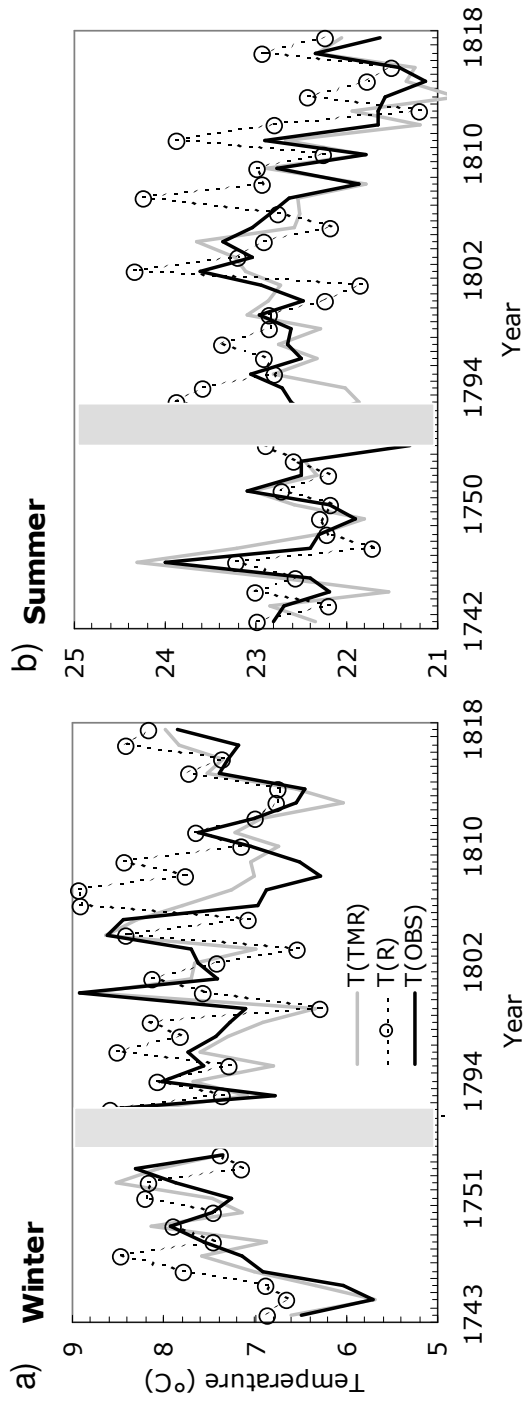
593 **Fig. 2.** Geometric interpretation of monthly values of the Temperature Anomalies Scale Index (*TASI*) for winter and summer (see Table 1a for  
 594 details). Black line: mean seasonal temperatures; red lines: reference values for positive temperature anomalies; blue lines: reference values for  
 595 negative temperature anomalies.  
 596  
 597



598 **Fig. 3.** Nomogram chart illustrating the multiresponse for different  $\Sigma TASI$ -values originating from regional temperature ( $T_R$ ) in (MTR)-model  
 599 for winter (a) and summer (b) (mathematical functions graphed using provisions supplied by GraphFunc-tool,  
 600 [http://www.seriesmathstudy.com/sms/graphfunc1\\_4x](http://www.seriesmathstudy.com/sms/graphfunc1_4x)).  
 601

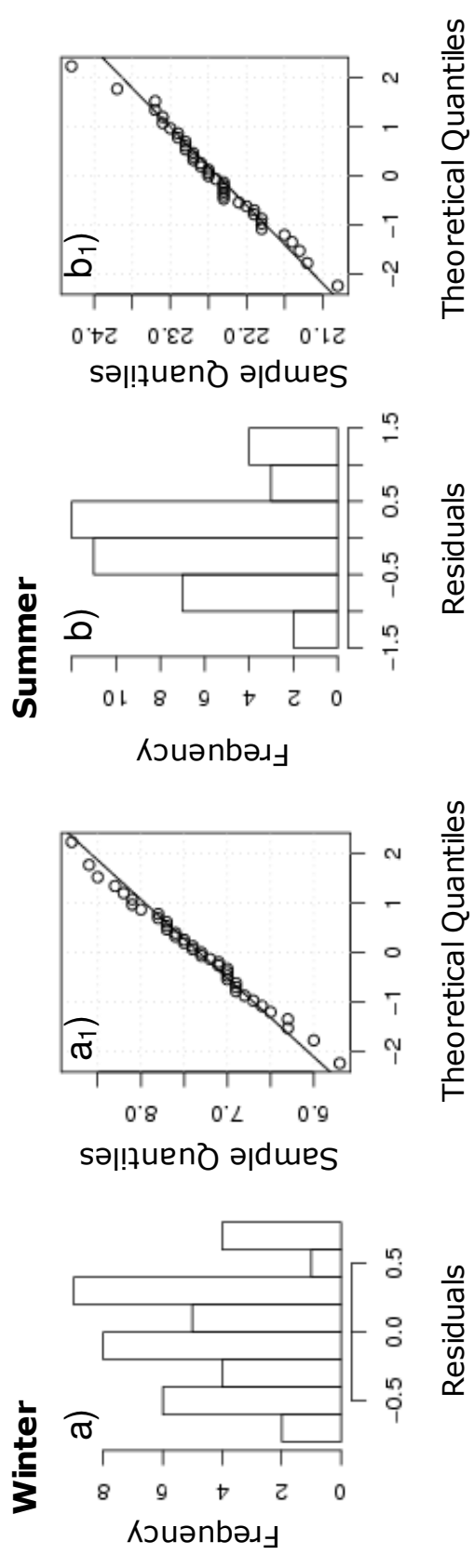


602 **Fig. 4.** Scatterplots between observed and predicted mean temperatures (°C) for Mediterranean Sub-regional Area (MSA) in winter (a) and in  
 603 summer (b) by (MTR)-model (Eq. 1). Diagonal lines 1:1 and outer dashed bounds at 95% prediction limits are drawn too.  
 604



606 **Fig. 5.** Trend of observed (black line: Camuffo et al., 2010), predicted by (MTR)-model (grey line), and by the regional model (circles:  
 607 Luterbacher et al., 2004) mean temperatures (°C) during 1742-1754 and 1772-1818, for winter (a) and summer (b), at validation stage.  
 608





609 **Fig. 6.** Histograms of residuals and QQ-plots of (MTR)-model (Eq. 1), during 1742-1754 and 1772-1818, for winter (**a, a<sub>1</sub>**) and summer (**b, b<sub>1</sub>**),  
610 respectively, at validation stage.  
611

a) Month	Categorical anomalies					Monthly TASI												Source
	Freezing	Very cold	Cold	Normal	Warm	Vary warm	Year	Dec	Jan	Feb	Jun	Jul	Aug	Winter	Summer			
Dec	-4	-2	-1	0	1	2	...	1	1	0	0	0	0	2	0	(A) (M)		
Jan	-4	-2	-1	0	1	2	1753	1	0	0	-2	0	0	1	-2	(A) (M)		
Feb	-4	-2	-1	0	1	2	1754	0	-1	0	0	0	-1	-1	-1	(A) (M)		
Jun	N/A	-4	-2	0	1	2	1755	0	-3	-1	-2	-2	-1	-4	-5	(A) (M)		
Jul	N/A	-5	-2	0	1	2	1756	0	0	-1	0	0	0	-1	0	(A) (M)		
Aug	N/A	-5	-2	0	1	2	1757	0	0	-1	-2	-2	0	-1	-4	(A) (M) (EVA)		

613 **Table 1.** Monthly-scaled index for decoding temperature anomalies from documentary proxy data (a) and temperature anomalies reconstruction  
614 for a selected number of years (b). Monthly values of the Temperature Anomalies Scale Index (TASI) are reported together with the seasonal  
615 sums ( $\Sigma TASI$ ) for winter (Win) and summer (Sum). Sources: A = *Corradi's Annals* (Corradi, 1850); M = *Moio and Susanna Manuscript* (Ferrari,  
616 1977); EVA = Catalogue EVA (Clemente and Margottini, 1991).

Scale of the estimation	Dataset	Performance statistics			Autocorrelation statistics		
		Nash-Sutcliffe efficiency coefficient	Correlation coefficient	Mean absolute error (°C)	Lag-1 residual correlation	Durbin Watson Statistic	
<b>Sub-regional (Eq. 1)</b>							
<b>Calibration</b>							
	Winter	0.88	0.94	0.24	0.27	1.45	( $p=0.02$ )
	Summer	0.87	0.88	0.24	0.04	1.83	( $p=0.23$ )
<b>Validation</b>							
	Winter	0.66	0.82	0.33	0.19	1.59	( $p=0.09$ )
	Summer	0.63	0.74	0.24	0.03	1.92	( $p=0.36$ )
<b>Regional (Luterbacher et al., 2004)</b>							
	Winter	-0.43	0.26	-	-	-	-
	Summer	-0.30	0.50	-	-	-	-

618 **Table 2.** Performance and autocorrelation statistics for (MTR)-model (Eq. 1) at the calibration and validation stages. Performance values over  
619 the validation set are also reported for the regional simulations.